Journal of the Serbian Society for Computational Mechanics / Vol. 18 / No. 1, 2024 / pp 124-138 / original paper
(10.24874/jsscm.2024.18.01.09)

FATIGUE ANALYSIS BASED ON FATIGUE FAILURE APPROACH AND DAMAGE TOLERANT APPROACH IN CORONARY STENT DESIGN

Gordana Jovičić[1] [0000-0002-9799-5555], Aleksandra Vulović[1,2*] [0000-0002-6726-3134], Arso Vukićević[1] [0000-0003-4886-373X], Nenad Đorđević[3] [0000-0002-2729-5721] and Nenad Filipović[1,2] [0000-0001-9964-5615]

[1] Faculty of Engineering, University of Kragujevac, Sestre Janjic 6, 34000 Kragujevac, Serbia
[2] Bioengineering Research and Development Center (BioIRC), Prvoslava Stojanovica 6, 34000 Kragujevac
[3] Centre for Assessment of Structures and Materials under Extreme Conditions, Brunel University London, Uxbridge, Middlesex UB8 3PH, United Kingdom
e-mail: gjovicic.kg.ac.rs@gmail.com, aleksandra.vulovic@kg.ac.rs, arso_kg@yahoo.com, Nenad.Djordjevic@brunel.ac.uk, fica@kg.ac.rs
**corresponding author*

Abstract

Over the last few decades, cardiovascular stents have emerged as crucial biomedical devices. Stents undergo cyclic physiological loading, which can lead to progressive accumulation of structural damage over time eventually resulting in a stent fracture. Considering the critical role of stents, it is necessary to assess their fatigue endurance and predict a potential premature failure due to fatigue loading. This paper presents a comprehensive analysis of coronary stent design based on both fatigue failure and damage-tolerant approaches. Employing the fatigue failure approach, S-N analysis was conducted to pinpoint the critical zones of the stent. Initial resistance to fatigue was evaluated using Goodman's and Soderberg's criteria. These criteria were applied to principal and effective stresses obtained using the Finite Element Method. Susceptibility to fatigue damage was performed by simulating the initial crack growth, and it was assessed through the Paris power law. The damage-tolerant approach yields more conservative fatigue stress ranges compared to fatigue failure criteria, ensuring safety under standard physiological loading conditions. The presented approach offers reliable insights into stent durability, with potential for further enhancement.

Keywords: Coronary stent, fatigue failure index, fatigue criterion, lifetime prediction.

1. Introduction

Cardiovascular stents have emerged as one of the most important biomedical devices over the last few decades. During their exploitation, they are subjected to cyclic physiological loading, which is why analysis of fatigue behavior is a critical step in the stent design, as the fatigue endurance strength of a material is typically significantly lower than its ultimate tensile strength. Due to fatigue, a progressive damage and stable fatigue failure crack growth can develop up to

the stent fracture. Based on the available data, it is estimated that 80-90% of stent failures are the result of a gradual accumulation of fatigue damage (Campbell, 2012). Consequently, the fatigue endurance assessment of biomedical devices is necessary to predict a potential for premature failure due to fatigue loading. The fatigue endurance assessment aims to determine the device's resilience against fatigue-induced failure. To ensure acceptable reliability and avoid fatigue fracture in critical devices like cardiovascular stents, the design safety from failure concept is developed.

A cardiovascular stent is designed to endure pulsating loading, applied at a heart frequency of 1.2 Hz, which corresponds to average of 70 load cycles per minute. These load cycles represent systolic-diastolic pressurization. The average frequency of 70 times per minute corresponds to 40 million cycles annually, or 400 million cycles over anticipated 10-year lifespan of a stent, as stipulated by the ASTM F2477-06 standard (ASTM, 2017). This standard sets the criteria for determining fatigue endurance of a stent, ensuring its resilience throughout its intended period of use.

It is well known that fatigue performance is sensitive to the size effects and predicting fatigue in the small structures using standard fatigue tests is challenging. Furthermore, conducting accelerated cardiovascular stent fatigue experiments is time-intensive, requiring approximately 6 months to complete 400 million cycles. To address these challenges, a current method for assessing reliability and durability of a cardiovascular stent is based on numerical calculation of the Fatigue Safety Factor (FSF) using Finite Element Analysis (FEA). These calculations rely on a comprehensive understanding of material fatigue properties. A cardiovascular stent is deemed reliable when the FSF is greater than one, or when the Fatigue Failure Index (FFI) is less than one, with FFI being an inverse of FSF. This approach represents a quantitative measure of safety and resilience against fatigue-induced failure in the stent design.

FEA is a numerical methodology that has found wide application for evaluating the mechanical behavior of stents (Miglivacca et al. 2002; Gervaso et al. 2008), stent design (Lally et al. 2005; Lally et al. 2006; De Blue et al. 2008) and Fatigue Failure Assessment of biomedical devices (Marey et al. 2006; Argente dos Santos et al. 2012). For instance, simulation of physiological and hyperphysiological loading conditions of the stent was conducted in Donnelly et al. (2007) and Pelton et al. (2008), whilst simulation of the extreme loads that appear during the stent deployment was published in Marey et al. (2006). Some authors used a full stent model (Marey et al. 2006; Argente dos Santos et al. 2012), whilst others used a unit cell model with appropriate application of periodic boundary conditions (Donnelly et al. 2007; Pelton et al. 2008).

Gong et al. (2009) presented an overview of methodologies for successful durability analysis of endovascular devices, including a Fatigue-Failure Approach. This approach involves a systematic series of steps:

- Conducting an experimental fatigue test on 8-12 samples exposed to constant radial distension, aimed at simulating physiological loading under clinical conditions for approximately 400 million cycles;
- Determining both tensile strength (σ_u) and fatigue endurance strength corresponding to 400 million cycles (σ_{400M});
- Fatigue calculation based on FEA where the mean stress and amplitude are calculated based on extreme stress values during cyclic loading;
- Calculating FSF using the fatigue failure criterion, considering a mean survival value (50%) and a reliable survival value of 90-95% of the projected lifespan;

- Estimating the radial distension of the stent, typically indicated by the worst-case scenario. This distortion can result from cyclic physiological loading or the interaction of the artery wall with the stent.

Following these steps, the Fatigue-Failure Approach for endovascular devices provides valuable insights into their performance within realistic clinical conditions. It should be noted that, in clinical practice, apart from systolic and diastolic physiological loads, various other forms of cyclic loads exist, as highlighted by Harewood et al. (2007). However, they are not included in the benchmark tests proposed in the literature (Gong et al. 2009).

The FSF and/or FFI approaches rely on fatigue criteria derived from numerically calculated stress states using FEA. The quantification of FSF and/or FFI can be achieved through the stress-based constant life approach, employing S-N analysis (Jovicic et al. 2014).

The fatigue-failure approach for stents can be summarized in the following steps:

- Experimental determination of stent's material properties: elasticity modulus, yield strength, tensile strength, and fatigue characteristics of the material for the specified lifetime of the stent corresponding to 400 million cycles (σ_{400M});
- Stress analysis using FEA: determining normal stress state - the most conservative or so-called worst-case scenario for cyclic physiological loading as well as other hyper-physiological states that can lead to accumulation of damage;
- I-fatigue analysis: calculation of FSF and/or FFI for a given physiological load;
- II-fatigue analysis: formation of a family of constant fatigue life curves for 10^8, 10^7, 10^6 load cycles; defining the mean and/or amplitude stress to achieve previous life cycles.

The approach described above is based on fatigue life prediction and has found wide application in biomedical engineering. This approach has been used by many authors (Nalla et al. 2003; Ritchie et al. 2006; Marrey et al. 2006a) and belongs to the conservative approaches that are based on the use of the Paris power law when assessing the integrity of a stent.

In this paper, a combination of fatigue failure and a damage-tolerant approach was used to assess the durability of a cardiovascular stent. Within the fatigue failure approach, it was assumed that there was no initial damage to the stent. At the same time, damage-tolerant life prediction requires an assessment of the integrity of the stent to the initial damage. The calculation of the stent fatigue was based on FEA, with the mean stress and amplitude stress calculated based on the extreme stress values during cyclic loading.

2. Geometric, boundary conditions, and material properties of the stent

In this study, we considered the structural configuration of the stent with a lower radial stiffness and geometry described in Jovicic et al. (2014). Material of the stent is L-605 Co-Cr, with the properties given in Marrey et al. (2006a).

The stress state of the stent results from cyclic blood pressure and physiological contact pressures against the artery walls. The length of the analyzed stent was 7mm, with an inner diameter of 1.5mm before deployment and an outer diameter of approximately 1.6mm (Fig. 1a). Dimensions of the rectangular cross-section of the stent are 0.08mm in the radial direction of 0.1mm in the circular direction.

The stent model was discretized using a structural hexahedral mesh comprising of 38400 nodes and 59625 elements. The stent was expanded from the initial diameter of 1.5 mm to 3 mm,

by a pressure of 1.8 MPa applied to the stent's internal faces. The stent's geometry provides lower radial stiffness and consequently lower stress levels in the radial direction. The boundary conditions were implemented in two steps (Fig. 1b). The areas where pressure loads were applied are shown in red color.

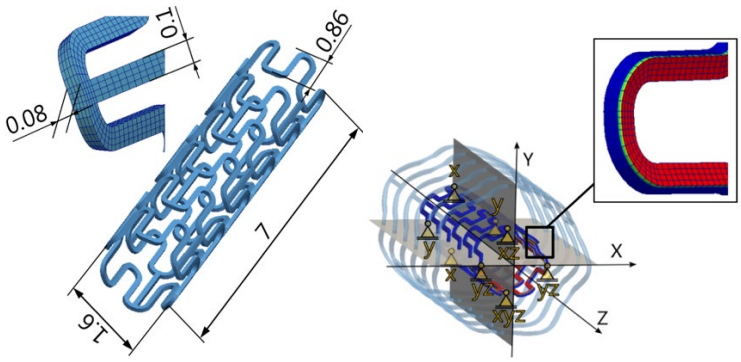

Fig. 1. Sketch of a) stent geometry; b) boundary conditions and zone of loads

Material properties for the high-quality L-605 Co-Cr alloy are given in Table 1 (Marrey et al. 2006a) and consist of standard material properties determined from static tests (first three) and the fatigue endurance strength limit that is determined in the fully reversed axial strain-controlled fatigue test.

Young's modulus E	Yield strength σ_y	Tensile strength σ_u	Fatigue endurance strength limit $\sigma_{400M}/2$	Threshold range ΔK_{th}^0	Paris fatigue parameters C, m
243 GPa	547 MPa	1449 MPa	207 MPa	2.58 $MPa\sqrt{m}$	$4.74 \cdot 10^{-13}$,10.39

Table 1. Material properties of L-605 Co-Cr

The fatigue ratio, representing the relationship between fatigue endurance strength and tensile strength of a material, is typically within the range of 0.25 to 0.6. For the adopted stent alloy L-605 Co-Cr, the fatigue ratio is chosen to be 0.286. Fatigue threshold range ΔK_{th}^0, ($MPa\sqrt{m}$) in Table 1 is determined experimentally.

In the context of biomedical devices, defects are often small cracks, typically smaller than ten micrometers (ASTM, 2006). The initial value for the fatigue threshold range for small cracks is the stress intensity factor, obtained at a crack growth rate of 10-10 m/cycle (Robertson et al. 2008). The initial value of the fatigue threshold range for small crack, ΔK_{th}^{sc} was determined based on the Paris fatigue parameters C and m:

$$\Delta K_{th}^{sc} = \left(\frac{10^{-10}}{C} \right)^{1/m} \tag{1}$$

Fatigue threshold range for small crack (ΔK_{th}^{sc}) is a critical parameter in initiating crack growth within structures such as cardiovascular stents. For the chosen alloy L-605 Co-Cr, the

fatigue threshold range for small cracks is $1.674MPa\sqrt{m}$, which is 1.54 times less than the experimental value given in Table 1. This deviation underscores the significance of initial cracks development in the cardiovascular stents and emphasizes the necessity of employing small crack theory in assessing their service life.

The majority of experiments determining the fatigue characteristics of materials involve fully reversed loading, where the load ratio is $R = \sigma_{min}/\sigma_{max} = -1$ (Fig. 2), where σ_{max} and σ_{min} are the maximum and minimum stress values in one load cycle, respectively, and the mean stress is $\sigma_m = 0$. The most commonly used standards for determining cyclic material properties include ASTM E606, the Recommended Practice for Strain-Controlled Fatigue Testing, and ISO12106, which refers to Metallic materials - Fatigue Testing- Axial-Strain-Controlled-Method.

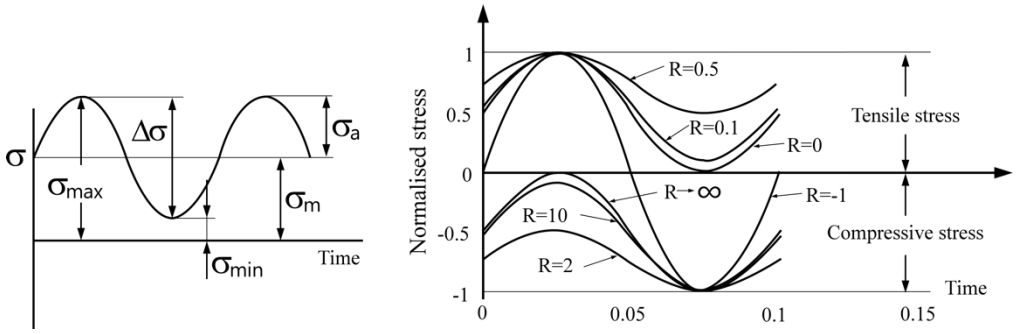

Fig. 2. Cyclic load forms of constant amplitude

It was experimentally determined that the fatigue threshold range for small cracks depends on the form of the load, specifically on the load ratio $R = \sigma_{min}/\sigma_{max}$, which has to be taken into account in predicting the fatigue life of the cardiovascular stents.

3. Damage-tolerant approach

The damage-tolerant approach is a conservative methodology employed to estimate the structural fatigue lifetime, based on the Paris power law (Marrey et al. 2006b). The fatigue failure, as shown in Fig. 3, can be divided into three phases generally, although the characteristics and duration of these phases primarily depend on the material subjected to cyclic loading.

The process of fatigue-induced damage typically unfolds through the following stages: a) nucleation of micro-cracks – small cracks a_0^{sc}; b) micro-crack growth a_0^{sc} up to the initial value a_0 (zone I); c) stable macro-crack growth from the initial value a_0 to the critical value a_c (zone II); d) unstable macro-crack growth, above the critical value a_c (zone III). While certain materials may exhibit robust resistance to crack nucleation, micro-crack growth, or macro-crack growth, it is rare for a material to possess all three resistances simultaneously.

Understanding these stages is essential for assessing the structural integrity and predicting the fatigue life of materials subjected to cyclic loading.

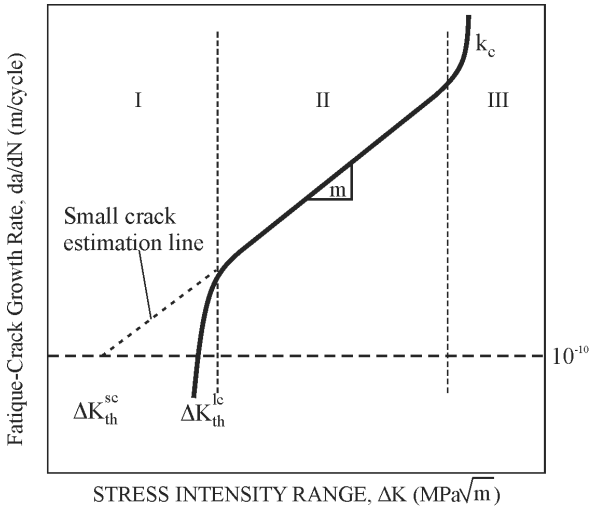

Fig. 3. Fatigue Crack growth rate vs Stress Intensity Range

Paris power-law on fatigue crack growth is defined as:

$$da / dN = C\left(\Delta K\right)^m \tag{2}$$

Paris power-law is effective in predicting stable crack growth (Zone II in Fig. 3), but it falls short in forecasting fracture during phase unstable crack growth ($da/dN \to \infty$). Unstable crack growth occurs when the stress intensity factor range reaches the fracture toughness $\Delta K \to K_c$. This critical value of the stress intensity range accounts for both material strength and its resistance to fracture under external loading.

A key limitation of Paris power-law (equation 2) is its failure to account for alternating load/stress and mean load/stress amplitude. The impact of the mean stress on fatigue crack growth rate is typically incorporated through the stress ratio R. Elber and Schjive (Elber 1970; Schjive 1981) addressed this deficiency by modifying Paris power-law and introducing the stress ratio in defining the stress intensity range, as:

$$\Delta K_{eff} = \left(0.55 + .33R + 0.12R^2\right)\Delta K \tag{3}$$

Applying this modified Paris power-law accounts for the load ratio effects and reduction in crack growth rate due to plasticity effects at the moment of crack closure.

3.1 Theory of small cracks

For the analysis of fatigue life of the cardiovascular stents, the most significant is crack initiation zone of the fatigue crack growth diagram (Fig. 3). This Zone I typically lasts the longest and is governed by the theory of small cracks. The crack initiation zone is best described by the Kitagawa-Takahashi (KT) diagram, which combines fatigue and fracture theories. Fig. 4 schematically shows the safe fatigue zone defined by the KT-diagram, which is defined by line A-B-C.

Below the A-B line, the crack has yet to reach its initial size a_0, and the laws of continuum mechanics and crack theory cannot be applied to it in standard engineering practice. This stage of the crack is referred to as the transient crack size. At point B, a transient crack size reached a_0,

which corresponds to the toughness threshold ΔK_{th}^{0}. The safe fatigue zone persists during the propagation of the initial crack, as long as cyclic loads remain below the line B-C.

However, a fracture occurs when stress states exceed the range corresponding to yield stress under pulsating fatigue loading, particularly when the crack has not yet reached the transient crack size (states above line A-B in Fig. 4). This underscores the critical role of understanding crack initiation and the crack growth, particularly in managing the durability of cardiovascular stents.

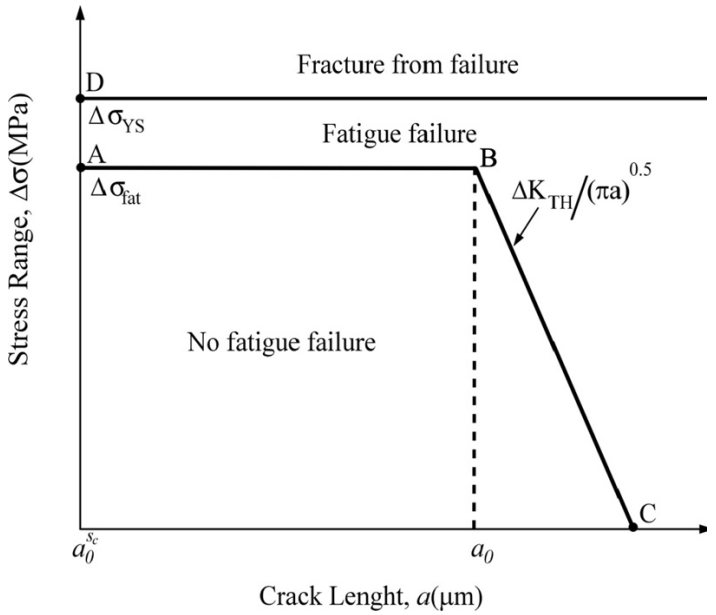

Fig. 4. K-T diagram and the safe zone under the cyclic-fatigue loading based on the theory of small cracks

The transient crack size denotes the threshold below which small crack effects significantly influence crack behavior, according to the Theory of Small Cracks (Fig. 4). If the size of the flaw is below the transient crack size a_0, then the fatigue threshold range is variable and can be approximated as a function of the size of the flaw by the relation:

$$\Delta K_{th}^{sc}\left(a\right) = Y\Delta\sigma\left(\pi a\right)^{1/2} \tag{4}$$

where $\Delta\sigma$ is the stress range, and Y represents the fatigue crack growth constant. The transient crack size, determined by the intrinsic material threshold range as shown in Table 1, is defined as follows:

$$a_0 \approx \frac{1}{\pi}\left(\frac{\Delta K_{th}^{0}}{Y\Delta\sigma}\right)^{2} \tag{5}$$

In relation 5, ΔK_{th}^{0} is the maximum value of the fatigue threshold range, which represents the intrinsic material threshold for a given material and is independent of crack size—whether long or small (Sadamanda et al. 2009). Therefore, it can be considered that the intrinsic material threshold range ΔK_{th}^{0} is constant if the flaw size is above the value of a_0. If the value of the

transient crack size a_0 is approximately equal to the value of one of the cross-sectional dimensions of the structure, the structure can be considered sensitive to fatigue and damage initiation (Lally et al. 2005).

4. Fatigue Failure Approach

Fatigue Failure Approach is based on defining the safety margin, denoted as FSF, through S-N analysis, under the assumption that no initial flaws exist in the structure. To evaluate FSF, it's essential to establish the amplitude stress and mean stress values for the adopted radially pulsating cyclic loading at each integration point from the finite element analysis. The amplitude stress during one load cycle is denoted as $\sigma_a = (\sigma_{max} - \sigma_{min})/2$, while the mean stress is defined as $\sigma_m = (\sigma_{max} + \sigma_{min})/2$. The extreme stress values $(\sigma_{max}, \sigma_{min})$ correspond to stress values during systolic and diastolic phases of pulsating cyclic loading. Fatigue failure will not occur if the amplitudes and mean stresses meet the conditions for the two fatigue theories:

$$\text{Goodman's: } \sigma_a / \left(\sigma_{400M} / 2\right) + \sigma_m / \sigma_u \leq 1 \tag{6}$$

$$\text{Soderbergh's: } \sigma_a / \left(\sigma_{400M} / 2\right) + \sigma_m / \sigma_y \leq 1$$

The fatigue endurance strength of the L-605 Co-Cr alloy should ensure the fatigue life of the stent for 400 million cycles of pulsating physiological loading. Therefore, for the L-605 Co-Cr alloy stent, the fatigue endurance limit corresponding to the designed number of cycles is $\sigma_{400M} = 0.286\sigma_u$ (Table 1).

If the inequality in relation 6 is met, then the structure is considered safe against failure for the designed period of 400 million load cycles. Therefore, the left side of relation 6 can be regarded as the Fatigue Failure Index. Achieving a design life of 400 million cycles corresponds to the equality in the relation 6. Inverse of the left side of relation 6 represents the Fatigue Safety Factor. Fatigue failure criteria specified by relation 6 account for the influence of the mean stress σ_m on the lifetime which is crucial for stents as physiological cyclic loading in the blood vessel involves high mean stresses and low amplitude stresses. In general, the impact of the mean stress on lifespan due to cyclic loading is depicted in Fig. 5.

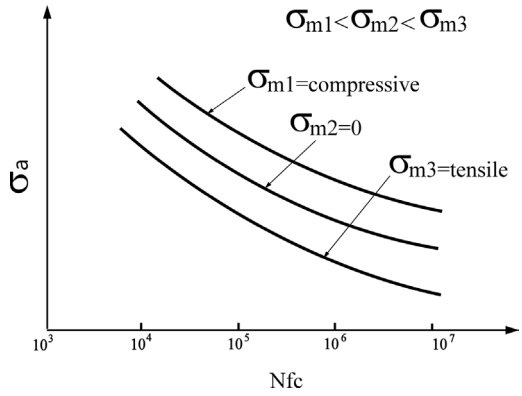

Fig. 5. Effect of mean stress on lifetime

In the assessment of fatigue failure safety, the extreme stress values for one load cycle correspond to systolic and diastolic blood pressure. The adopted variation between systolic and

diastolic blood pressure in the artery are typically 100 mmHg (approximately 13.3 kPa) (Lally et al. 2005). Numerically calculated maximum stress values within the stent for the two blood pressures that constitute one load cycle were used for computing the FFI. Numerical results were obtained from using in-house FEM modeling software PAK (Kojic et al. 2005).

Fig. 6 shows the principal stress distribution for systolic physiological blood pressure. The FEA shows that the T-zone of the stent is subjected to extreme stress values. The T-zone refers to the junction of the stent bridge and the stent strut.

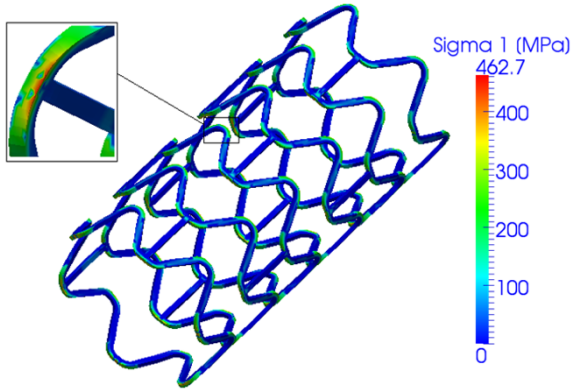

Fig. 6. The principal stress distribution for the higher blood pressure

Fig. 7 shows the amplitude and mean stress values for one load cycle in the T-zone of the stent.

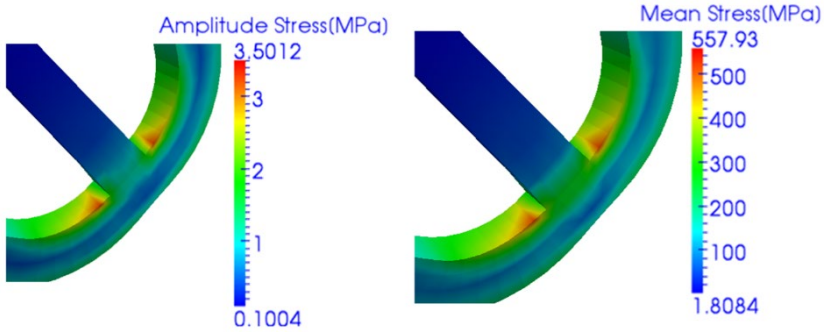

Fig. 7. Amplitude and mean stress for one loading cycle in the T-zone of the stent

Fig. 8 shows the distribution of the FFI across the critical zones of the stent based on Soderberg's criterion. The amplitude and mean stress used for defining the FFI, were calculated using the principal stress Sigma1, obtained at the elements' Gaussian points.

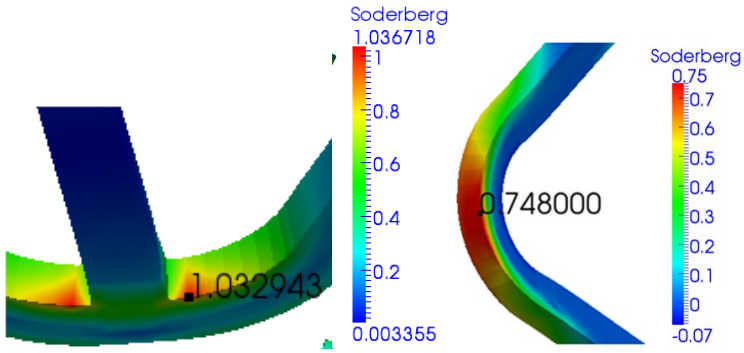

Fig. 8. FFI distribution obtained by applying Soderberg's fatigue failure criterion

According to the fatigue criterion, the critical sites for failure are in areas of geometric stress concentration, specifically the T-zone and the region with the smallest radius. The highest FFI according to Soderberg's criteria appears in the T-zone. This criterion is more conservative than Goodman's because it uses yield strength as a measure of fatigue failure for mean stress, rather than UTS used in Goodman theory. Soderbeg's criterion essentially defines linear-elastic behavior as the limit for fatigue failure. The critical value of FFI=1.0329 according to Soderberg's fatigue criterion corresponds to a lifetime of 400 million fatigue life cycles.

5. Worst-Case Prediction Analysis in Fatigue Failure Approach and Damage Tolerant Approach

The calculation points with the highest FFI values (Fig. 8) pose the greatest risk of failure. A worst-case prediction analysis was conducted based on the numerical stress values in these zones, considering constant fatigue life values of 400 million cycles, 10 million and 1 million cycles (Gong et al. 2009). It is important to note that there is not a universally standardized approach for defining the physiological worst-case scenario in the literature. Adopting extremely conservative loads for the worst-case scenario, coupled with poor material properties and unfavorable geometry, may result in oversizing of the stent.

Fig. 9 shows the scenario of unfavorable physiological conditions leading to fatigue failure at 400 million cycles, where the numerical worst-case (σ_a^N, σ_m^N) is marked with a star. Three different scenarios of the physiological worst-case loading were considered in this study, at a constant lifetime of 400 million cycles:

I. Retaining the numerical mean stress value while increasing the amplitude to the constant Goodman fatigue life diagram of 400 million cycles (corresponding to FSF=1)

II. Radially increasing both amplitude and mean stress from the numerical worst-case stress to the Goodman constant fatigue life diagram of 400 million cycles.

III. Maintaining the numerical worst-case value for amplitude stress while increasing the mean stress to the Goodman constant fatigue life diagram of 400 million cycles.

Let σ_a^N and σ_m^N denote, respectively, the amplitude and mean stress at the numerical worst-case point obtained at the Gaussian point with the highest FFI value. The obtained numerical worst-case solutions of $\sigma_a^N = 3.453MPa$ (scenario III) and $\sigma_m^N = 555.89MPa$ (scenario I) were very close to the value on Soderberg's constant life diagram corresponding to

400 million cycles. Table 2 presents the calculated mean and amplitude stress values for the three worst-case prediction scenarios (Fig. 9).

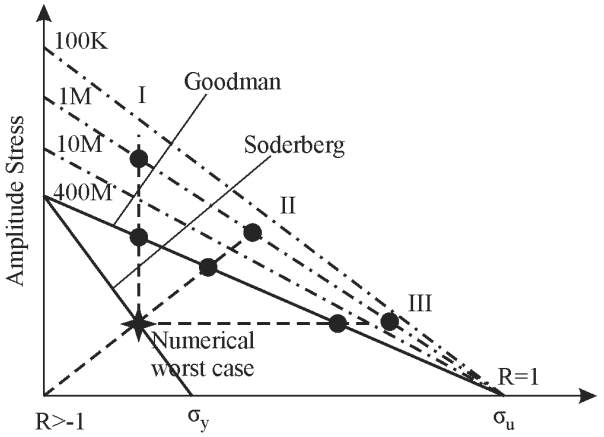

Fig. 9. Worst Case Prediction scenario I, II, III from constant fatigue lifetime of 400 million cycles

σ_m^I	σ_a^I	σ_m^{II}	σ_a^{II}	σ_m^{III}	σ_a^{III}
555.89 MPa	127.59 MPa	1388.4 MPa	8.62 MPa	1449 MPa	3.45 MPa

Table 2. Worst-Case Stress Scenario Prediction for constant Goodman fatigue life of 400 million cycles

The fatigue load stress range in the first worst stress scenario is $\Delta\sigma = 255.2$ MPa, which is ≈61% of fatigue endurance stress limit for L-605 Co-Cr material. The second scenario gives a mean stress of 1388.4MPa, which is ≈96% of the tensile strength of the material. The third scenario gives a mean stress of 1449MPa which is equal to the tensile strength of L-605 Co-Cr. In the second and third scenarios, the values of the fatigue load stress range are within acceptable limits, while the mean stress is at the limit of the endurance of the material.

The obtained worst-case values for fatigue load assume no flaws in the stent structure. The high value of the fatigue load stress range in the first worst-case scenario by far exceeds physiological conditions, suggesting that, for this stent configuration, it can be treated as an instantaneous load rather than a fatigue load. In Case II and Case III, the mean stress approaches the Ultimate Tensile Strength, suggesting conditions closer to monotonic loading rather than typical cyclic loading observed in physiological conditions.

All three worst-case scenarios were defined for a design life of 400 million load cycles. The assumed physiological loading conditions result in mean stresses below those shown in Table 3, indicating structural tolerance to fatigue, assuming no initial damages. However, initial damage to the stent may occur during its deployment.

To assess tolerance to fatigue damage, it is necessary to assume the existence of a flaw in the form of a transient crack size. For the selected alloy L-605 Co-Cr, the intrinsic material threshold is $\Delta K_{th} = 2.58 MPa\sqrt{m}$, while the transient crack size based on relation 4 is: $a_0 = 9.8\mu m \approx 10\mu m$. The transient crack size is adopted as a shallow flaw worst-case scenario. If the transient crack size exceeds the dimensions of the stent's cross-section, it indicates sensitivity to fatigue with a specific fracture form (Marrey et al. 2006a).

Using the Paris power-law of fatigue crack growth, fatigue life was predicted by defining the number of loading cycles as a function of flaw size and stress range, assuming stable crack growth (Region II in Fig. 3). This analysis was performed for different levels of fatigue load stress range, with the projected lifetime of 400 million load cycles taken as a measure of the structure's critical condition.

Fig. 10 shows the projected lifeline obtained by applying the damage life approach, showing the critical crack length versus the fatigue load stress range, obtained by using Paris law. At a physiological stress range <20 MPa (Fig. 10), the designed life of the structure is achieved for a shallow crack size ≥230 μm that by far exceeds the cross-sectional dimensions of the stent. Moreover, by applying the fatigue growth law and considering the projected lifetime of the stent structure, the critical value of the fatigue load stress range can be determined, leading to the critical crack size. The critical crack value here would be considered a dimension equal to one of the cross-sectional dimensions of the stent.

The designed life of the stent would be reached by the crack formation that corresponds to the smaller dimension of the cross-section of the stent if the fatigue load stress range was 45MPa. For a fatigue load stress range of 40 MPa, the critical value of the crack would be overcome by a larger stent cross-sectional dimension of 100μm.

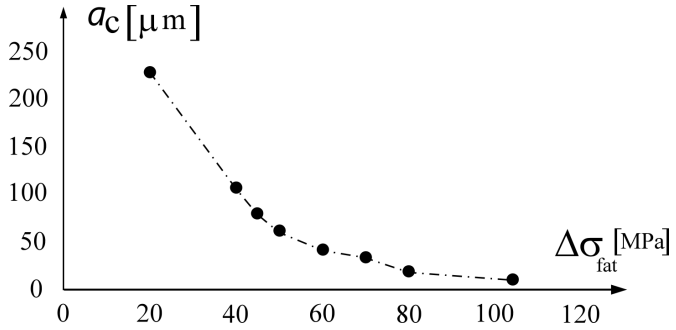

Fig. 10. The line of the stent's designed life - damage tolerant fatigue approach.

$\Delta\sigma_{fat}$ $[MPa]$	20	40	45	50	60	70	80	104
$a_c[\mu m]$	>230	107,9	80,57	62,1	42.1	34,2	19,38	10

Table 3. Critical size flaw for different values of the fatigue stress range at which the projected lifetime is achieved

The last value of the stress range in Table 2, 104 MPa, corresponds to the maximum crack growth, which aligns with the crack size of 10μm. This value of the fatigue load stress range significantly surpasses the pulsating physiological stress range and may potentially occur during the stent's deployment process within the anatomical location of the blood vessel. Consequently, such values of the fatigue load stress range for this stent's structural configuration can be regarded as instantaneous loads rather than fatigue loads.

Given the above, the considered structural configuration would be deemed safe according to conservative failure criteria under the influence of instantaneous overload if the extreme local values of the fatigue load stress range remain below the experimentally determined toughness value. This condition was quantified through the FFI in the previous chapter. Table 5 illustrates the relationship between crack growth rate under the Modified Paris law and Paris law for different stress ratio values R. For instance, at a stress ratio value of R = 0.625, equivalent to a

blood pressure ratio of 100Hmmg/160Hmmg, the crack growth rate is only 10.2% of the value obtained by relation (2).

R	0.125	0.25	0.5	0.625	0.75	1
$(da/dN)^{\dagger}/(da/dN)^{\ddagger}$	0.0044	0.0097	0.047	0.102	0.22	1

† Modified Paris law; ‡ Paris law

Table 4. Crack growth rate ratio of Modified Paris law and Paris law

The previous table shows a decrease in the crack growth rate, attributable to the crack closure effect, which is taken into account through the stress ratio in the modified Paris law (see equation 3). The high resistance of the L-605 Co-Cr material to fatigue crack growth is primarily reflected in the value of the Paris exponent m, which is, for this alloy, equal to 10.39, whilst for most ductile materials it ranges from 2 to 4 (Ritchie, 1999). When considering the material's plasticity and the subsequent crack closure effect, the rate of crack propagation is significantly decelerated, thereby extending its lifespan. This decelaration of the crack growth is significant while there is Small Scale Yielding (SSY). However, in the phase when significant flow occurs (significant zone of plasticity) in the vicinity of the crack tip, the difference in crack growth simulation using relations (2) and (3) decreases.

6. Conclusions

The paper presents the analysis of coronary stent design employing both fatigue failure and damage-tolerant approaches. In the fatigue failure approach, critical zones of the stent are identified through S-N analysis, based on FFI and/or FSF, without presence of initial damage within the structure.

Typical physiological loads on a coronary stent are characterized by small load amplitudes, resulting in low values of fatigue load stress range compared to mean stress values. These physiological worst-case scenarios often manifest as extreme hypertension.

Soderberg's criterion defines the critical line of constant life for 400 million cycles based on yield stress, without tolerating residual stress occurrence. Worst-case scenarios for the stent's projected lifetime are created using Goodman's fatigue criteria, significantly exceeding physiological conditions, thus ensuring a wide tolerance for fatigue failure assuming an absence of initial flaws.

Fatigue stress ranges obtained with the damage tolerant approach were significantly more conservative than those predicted by the fatigue failure criteria. Both analyses confirm the safety of the chosen design geometry/stent material under standard physiological fatigue loading conditions. For the fatigue failure approach, an extreme fatigue load stress range of approximately 250MPa was obtained for a projected constant lifetime of 400 million cycles. Meanwhile, for the damage tolerance approach, the maximum fatigue load stress range was 45 MPa for the larger cross-sectional dimension and 40 MPa for the smaller cross-sectional dimension of the stent, both significantly higher than physiological conditions.

The presented approach offers reliable results for assessing the structure's durability under fatigue load. Further improvements to the damage-tolerant approach should consider multiaxial physiological loading forms, necessitating inclusion of mixed-mode loading in numerical analyses and validation tests to reflect real arterial structures accurately.

Acknowledgements: The research was funded by the Ministry of Science, Technological Development and Innovation of the Republic of Serbia, contract number [451-03-65/2024-03/200107 (Faculty of Engineering, University of Kragujevac)].

References:

Argente dos Santos HAF, Auricchio F, Conti M (2012). Fatigue life assessment of cardiovascular balloon-expandable stents: a two-scale plasticity–damage model approach, *Journal of the mechanical behavior of biomedical materials*. 15, 78-92.

ASTM (American Society of Testing Materials) F2063-18 (2006). Standard specification for wrought nickel-titanium shape memory alloys for medical devices and surgical implants. ASTM Book of Standards v13.01.

ASTM (American Society of Testing Materials) F2477-06 (2017). Standard test methods for in vitro pulsatile durability testing of vascular stents. ASTM Book of Standards v13.01.

Campbell FC (2012). *Fatigue and Fracture: Understanding the Basics*, 1st ed. ASM International.

De Beule M, Mortier P, Carlier SG, Verhegghe B, Van Impe R, Verdonck P (2008). Realistic finite element-based stent design: the impact of balloon folding, *Journal of Biomechanics*, 41(2), 383-9.

Donnelly EW, Bruzzi MS, Connolley T, McHugh PE (2007). Finite element comparison of performance related characteristics of balloon expandable stents, *Computer Methods in Biomechanics and Biomedical Engineering*, 10(2), 103-110.

Elber W (1970). Fatigue crack closure under cyclic tension, Engineering Fracture Mechanics, 2(1), 37-45.

Gervaso F, Capelli C, Petrini L, Lattanzio S, Di Virgilio L, Migliavacca F (2008). On the effects of different strategies in modelling balloon-expandable stenting by means of finite element method, *Journal of Biomechanics*, 41(6), 1206-12.

Gong XY, Chwirut DJ, Mitchell MR, Choules BD, Cavanaugh K (2009). Fatigue to fracture: an informative, fast, and reliable approach for assessing medical implant durability, *Journal of ASTM International*, 6(7), JAI102412.

Harewood FJ, McHugh PE (2007). Modeling of size dependent failure in cardiovascular stent struts under tension and bending, *Annals of Biomedical Engineering*, 35, 1539-53.

Jovicic GR, Vukicevic AM, Filipovic ND (2014). Computational assessment of stent durability using fatigue to fracture approach, *Journal of Medical Devices*, 8(4), 041002.

Kojic M, Slavkovic R, Zivkovic M, Grujovic N, Jovicic G, Vulovic S (2005). *PAK-FM&F–Software for Fracture Mechanics and Fatigue based on the FEM and X-FEM*, Manual, University of Kragujevac, Kragujevac, Serbia.

Lally C, Dolan F, Prendergast PJ (2005). Cardiovascular stent design and vessel stresses: a finite element analysis, *Journal of biomechanics*, 38(8), 1574-81.

Lally C, Dolan F, Prendergast PJ (2006). Erratum to "Cardiovascular stent design and vessel stresses: A finite element analysis", *Journal of Biomechanics*, 9(39), 1760.

Marrey RV, Burgermeister R, Grishaber RB, Ritchie RO (2006). Fatigue and life prediction for cobalt-chromium stent: A fracture mechanics analysis, *Biomaterials*, 27, 1988-2000.

Marrey RV, de Almeida LH, Lobosco M (2006). Damage-tolerant assessment of the durability of a cardiovascular stent using the Paris power law, *Journal of Biomedical Materials Research Part B: Applied Biomaterials*, 79(1), 209-218.

Migliavacca F, Petrini L, Colombo M, Auricchio F, Pietrabissa R (2002). Mechanical behavior of coronary stents investigated through the finite element method, *Journal of biomechanics*, 35(6), 803-11.

Nalla RK, Imbeni V, Kinney JH, Staninec M, Marshall SJ, Ritchie RO (2003). In vitro fatigue behavior of human dentin with implications for life prediction, *Journal of Biomedical*

Materials Research Part A: An Official Journal of The Society for Biomaterials, The Japanese Society for Biomaterials, and The Australian Society for Biomaterials and the Korean Society for Biomaterials, 66(1), 10-20.

Pelton AR, Schroeder V, Mitchell MR, Gong XY, Barney M, Robertson SW (2008). Fatigue and durability of Nitinol stents, *Journal of the Mechanical behavior of Biomedical Materials*, 1(2), 153-64.

Ritchie RO (1999). Mechanisms of fatigue-crack propagation in ductile and brittle solids, *International Journal of Fracture*, 100, 55-83.

Ritchie RO, Kinney JH, Kruzic JJ, Nalla RK (2006). *Cortical bone fracture*, In Wiley Encyclopedia of Biomedical Engineering, John Wiley & Sons, 32–45.

Robertson SW, Ritchie RO (2008). A fracture-mechanics-based approach to fracture control in biomedical devices manufactured from superelastic Nitinol tube*, Journal of Biomedical Materials Research Part B: Applied Biomaterials*, 84(1), 26-33.

Sadananda K, Sarkar S, Kujawski D, Vasudevan AK (2009). A two-parameter analysis of S–N fatigue life using Δσ and σmax, *International Journal of Fatigue*, 31(11-12):1648-59.

Schijve J (1981). Some formulas for the crack opening stress level, *Engineering Fracture Mechanics*, 14(3), 461-5.